Water Vapor Vertical Profile Structures Retrieved from Satellite Data via Classification and Discrimination

ALAN E. LIPTON, DONALD W. HILLGER* AND THOMAS H. VONDER HAAR

Department of Atmospheric Science, Colorado State University, Fort Collins, CO 80523

(Manuscript received 24 April 1985, in final form 29 November 1985)

ABSTRACT

A method of retrieving the basic vertical structure of water vapor profiles from satellite-observed radiances is presented. The statistical tools of empirical orthogonal function analysis and clustering were used to define classes of vertical structure of water vapor. As a result, any water vapor sounding can be assigned to one of four vertical structure classes. Each class was shown to be identified with certain types of weather features. Multiple regression was used to retrieve approximate total precipitable water by use of brightness temperatures simulated for the Defense Meteorological Satellite Program SSH-2 infrared sounder, resulting in explained variances of about 80%. In addition, discriminant analysis was then applied to retrieve the vertical structure class of each water vapor profile, giving percentages of correct discrimination near 60%. Selection from among the SSH-2 spectral channels was used to optimize both the total water regression and the structure class discrimination. Also, it was shown that separation of soundings by total water content generally improves discrimination skill by a few percent. The results suggest that this retrieval approach should be particularly useful for application to subjective weather forecasting.

1. Introduction

Meteorologists and atmospheric modelers are interested in water vapor profiles primarily because they must evaluate the potential for cloudiness and precipitation. For their work, the most important aspects of profiles are the total precipitable water and the general shape of the profile. Thin layers of relatively high or low humidity are important in some situations, but are generally of secondary concern.

Research on retrieval of water vapor profiles from satellite data has shown that, under cloud-free conditions, total precipitable water can be retrieved with substantial accuracy (about 80% explained variance). Useful information about the basic profile structure is also available (Smith and Howell, 1971; Moyer et al., 1978; Gruber and Watkins, 1979; Hayden et al., 1981; Chesters et al., 1982; Hillger, 1984; Rosenberg et al., 1983). However, fine details of the water vapor vertical structure cannot be retrieved. The limitations on retrieval are rooted in radiation physics, which dictates that the current state-of-the-art sounders have very broad weighting functions in their water vapor-sensing channels (Wark et al., 1974). Profile detail will elude retrieval as long as sounder weighting functions are broad relative to the depth of the troposphere (Twomey, 1966).

In light of these considerations, we developed a quick-solution retrieval method based on the premise that water vapor retrieval skill is limited to the basic features of the profile, and if accurately determined, they describe the bulk of the meteorologically important information in the profile.

Most of the studies noted here involved retrieving water vapor parameters at several specific levels. An alternate approach is to directly retrieve information on the overall atmospheric structure. This approach has been applied to temperature sounding (Prabhakara et al., 1979; Uddstrom and Wark, 1985; Thompson et al., 1985), and we applied it to water vapor sounding.

Development of our water vapor retrieval procedure involved specifying what structures to look for in the vertical distribution of water vapor, and devising a method to recognize those structures by means of satellite-based measurements. The specification of water vapor structures was accomplished through empirical orthogonal function (EOF) analysis, clustering and classification. To accomplish the structure recognition, we used multiple regression to retrieve a parameter that approximates total precipitable water, and then discriminant analysis to retrieve water vapor vertical structure.

2. Data

Radiosonde observations (RAOBs) of temperature and water vapor concentration were the primary data base, and were used 1) to simulate satellite sounder

* Present affiliation: Cooperative Institute for Research in the Atmosphere (CIRA), Colorado State University, Fort Collins, CO 80523.

brightness temperatures (equivalent blackbody temperatures), 2) to determine characteristic vertical structures of water vapor profiles, and 3) together with the simulated brightness temperatures, to derive coefficients for statistical profile retrieval. We considered 360 RAOBs from the tropics (30°N–30°S) in all seasons (set TR), and 251 from midlatitudes (30°N–60°N) during the summer half-year (1 May–31 October) (set MLS). The RAOBs were launched from about 30 oceanic sites. The study was limited to oceanic soundings to avoid the complication of varying surface elevation, and because satellite-based sounding over oceans promises a great improvement relative to the sparse conventional sounding network.

The RAOBs were extensively screened for completeness and consistency. Also, for radiative transfer calculations, the RAOBs were extrapolated from the highest reported level up to 0.1 kPa by filling in values from the standard atmospheres supplied in LOWTRAN 5 (Kneizys et al., 1980).

Brightness temperatures were simulated for the Defense Meteorological Satellite Program (DMSP) Special Sensor H-2 (SSH-2) infrared sounder. Simulation was necessary because no real SSH-2 data were available during our investigation. The SSH-2 is designed to measure radiances in 16 spectral bands, as given in Table 1; weighting functions for the H_2O channels are in Fig. 1. The information content of the SSH-1 H_2O channels (which are very similar to those of SSH-2) was reported by Valovcin (1980).

Radiation was computed for cloud-free conditions, since the retrieval of water vapor concentration from infrared sounder data is severely limited by clouds. LOWTRAN 5 (Kneizys et al., 1980) radiative transfer software was used to compute brightness temperatures based on the SSH-2 spectral responses. The lower boundary was assigned a temperature equal to that of the lowest atmospheric level and an emittance of 1.0. Noise was added to the brightness temperatures from a normal distribution of random numbers. The amplitude of noise was specified by doubling the Noise Equivalent Spectral Radiances (NESR) measured by Barnes Engineering (1978b). NESRs are estimates of the standard deviation of instrument error. Simulations based on LOWTRAN 5 could not reflect the details of the SSH-2 spectral responses due to insufficient spectral resolution (20 cm^{-1}). Therefore, retrieval coefficients based on these simulations would have to be recomputed with real SSH-2/RAOB pairs of soundings before they could be applied in the field.

TABLE 1. SSH-2 channel characteristics (Barnes Engineering, 1978a,b).

Band	Central wavenumber (cm^{-1})	Halfwidth (cm^{-1})	Primary absorbing constituent
E1	668.5	3.0	CO_2
E2	677.0	12.5	CO_2
E3	695.0	12.5	CO_2
E4	708.0	12.5	CO_2
E5	731.0	12.5	CO_2
E6	747.0	12.5	CO_2
E7	797.0	12.5	H_2O
E8	898.0	12.5	window
F8	353.0	14.0	H_2O
F2	397.0	12.5	H_2O
F6	408.0	14.0	H_2O
F3	420.0	22.0	H_2O
F4	441.0	20.0	H_2O
F5	497.0	17.0	H_2O
F1	535.0	15.0	H_2O
W	2700.0	275.0	window

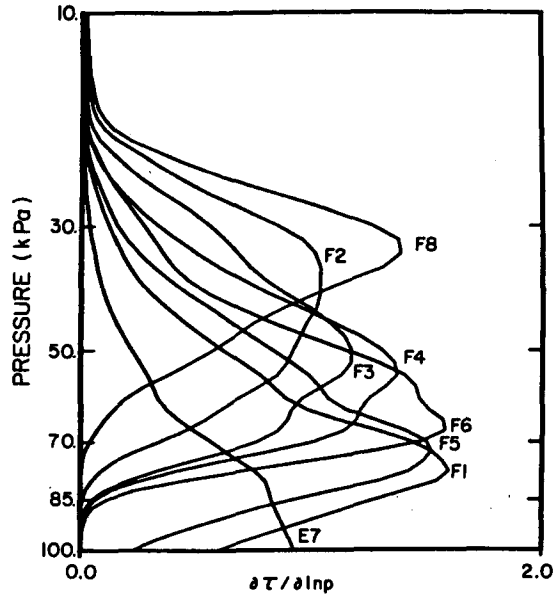

FIG. 1. Weighting functions $\partial\tau/\partial \ln p$ for the DMSP SSH-2 water vapor channels, as computed from a tropical model sounding [after Rosenberg et al. (1983)].

3. Determination of vertical structure classes

a. Decomposition of mixing ratio profiles

Empirical orthogonal function (EOF) analysis was used to evaluate the vertical structure of water vapor profiles. Precedents for an EOF approach include Koprova and Malkevich (1965), who used EOFs to characterize atmospheric temperature and moisture structure. The works of Jalickee and Ropelewski (1979), Uddstrom and Wark (1985) and Thompson et al. (1985) are related to ours in that they used similar means to classify temperature soundings according to vertical structure for satellite-based retrievals. We used an EOF-type approach because it is an efficient way to depict the coherent features in vector observations such as RAOBs.

For each RAOB set (TR and MLS), EOFs (eigenvectors) were computed from the mixing ratio covari-

ance matrix (Kendall, 1975). Each mixing ratio profile vector $\mathbf{q}$ was transformed into a principal component vector $\mathbf{c}$ following the relationship

$$\mathbf{q} = \mathbf{q}_m + \mathbf{E}\mathbf{c}, \quad (1)$$

where $\mathbf{q}_m$ is the mean profile for the set, and $\mathbf{E}$ is a matrix with each column composed of one eigenvector. The vectors were of length six, with each element corresponding to one of the RAOB mandatory reporting levels (30, 40, 50, 70, 85, and 100 kPa) for water vapor. Both $\mathbf{q}$ and $\mathbf{c}$ are specific to a single RAOB, while $\mathbf{q}_m$ and $\mathbf{E}$ are constant over a dataset.

The three-eigenvector approximation to (1) is

$$\mathbf{q} \approx \mathbf{q}_m + \mathbf{e}_1 c_1 + \mathbf{e}_2 c_2 + \mathbf{e}_3 c_3, \quad (2)$$

and is accurate to 98% for both TR and MLS datasets. The first principal component alone explains 79% and 77% of the mixing ratio variance for sets TR and MLS, respectively. The first three eigenvectors of set TR are plotted in Fig. 2 (those of set MLS were similar).

From the characteristics of $\mathbf{e}_1$ (monotonic, no change in sign) and the proportion of variance explained by c_1, we concluded that c_1 can be interpreted as the "overall wetness" of a profile, relative to the mean. Vectors $\mathbf{e}_2$ and $\mathbf{e}_3$ have vertical structure, with c_2 and c_3 giving the magnitudes of the primary structure-related components. Accordingly, (2) can be rewritten as

$$\mathbf{q} \approx \mathbf{q}_m + \mathbf{q}_w + \mathbf{q}_s, \quad (3)$$

where

$$\mathbf{q}_w = \mathbf{e}_1 c_1 \quad \text{(overall wetness part)}, \quad (4)$$

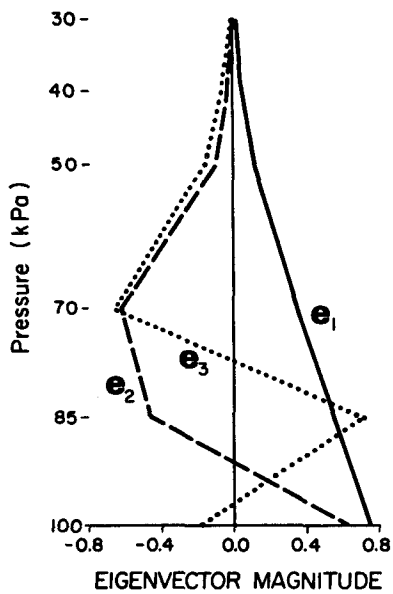

FIG. 2. The first three eigenvectors of the mixing ratio covariance matrix for dataset TR.

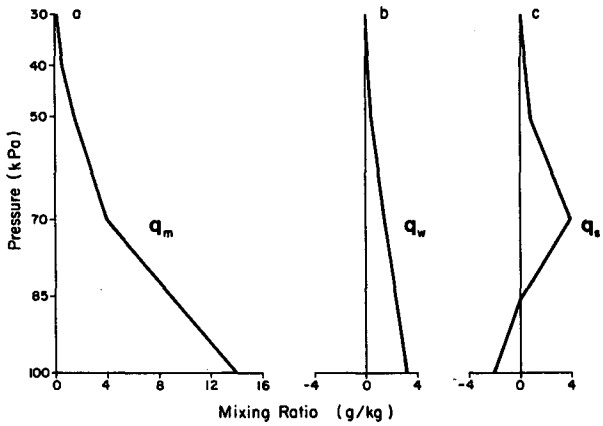

FIG. 3. A TR mixing ratio profile decomposed into its (a) mean, (b) overall wetness, and (c) vertical structure components.

and

$$\mathbf{q}_s = \mathbf{e}_2 c_2 + \mathbf{e}_3 c_3 \quad \text{(structure part)}. \quad (5)$$

Figure 3 shows one sample profile decomposed via (3). Looking towards retrieval of profile structures from satellite data, we choose to do further analysis on the structure parts of the soundings in our datasets.

b. Clustering and classification

Objective clustering (Kendall, 1975) was applied separately to the TR and MLS sets to determine classes of vertical structure. Our application of clustering (Vonder Haar et al., 1983) was designed to result in four classes. RAOBs with relatively high values of c_2 and high values of c_3 were put into one class, those with high c_2 and low c_3 formed another class, and so on (see Fig. 4). The high/low boundaries in c_2, c_3 space were drawn half-way between the "optimal" cluster centers, where optimal means that, given the Euclidean distance between each RAOB and its assigned cluster center, the ensemble sum of all distances is a minimum. We added the constraint that the boundaries be parallel to the c_2 and c_3 axes (Vonder Haar et al., 1983). Each cluster center (the circles in Fig. 4) can be interpreted as being characteristic of the vertical structure class (VSC) defined by the surrounding classification boundaries ($\bar{c}_2$ and $\bar{c}_3$). The boundaries can be used to identify which VSC any RAOB belongs to.

We found it useful to distinguish between soundings whose values of c_2 and c_3 put them close to the classification boundaries and those that were more clearly associated with a particular VSC. A borderline region was defined as the area within $\bar{c}_2 \pm \sigma_2/2$ and $\bar{c}_3 \pm \sigma_3/2$, where σ_2 and σ_3 are the standard deviations of c_2 and c_3, respectively (Fig. 4). Soundings outside that area were denoted as "distinctive."

When the coordinates of the cluster centers (c_2^+, c_3^+, etc., in Fig. 4) are input to (5) the results are vertical structure vectors that are characteristic of the VSCs;

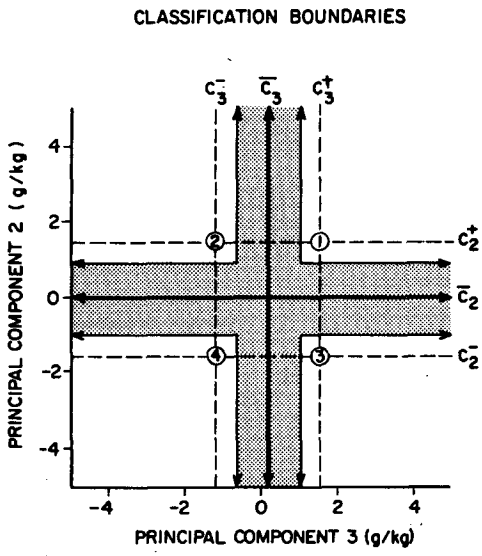

FIG. 4. A schematic illustration of clustering and classification for TR mixing ratio soundings. The circles indicate cluster centers, with the enclosed number identifying the associated VSC. The c_2^+, c_2^-, c_3^+ and c_3^- represent the coordinates of the cluster centers in c_2, c_3 space. The classification boundaries are designated $\bar{c}_2$ and $\bar{c}_3$. The shaded area represents the domain of borderline soundings, with distinctive soundings residing in the unshaded areas.

$$\mathbf{q}_{s1} = \mathbf{e}_2 c_2^+ + \mathbf{e}_3 c_3^+, \quad (6a)$$

$$\mathbf{q}_{s2} = \mathbf{e}_2 c_2^+ + \mathbf{e}_3 c_3^-, \quad (6b)$$

$$\mathbf{q}_{s3} = \mathbf{e}_2 c_2^- + \mathbf{e}_3 c_3^+, \quad (6c)$$

$$\mathbf{q}_{s4} = \mathbf{e}_2 c_2^- + \mathbf{e}_3 c_3^-. \quad (6d)$$

The four TR VSC-characteristic vectors are given in Fig. 5, while those for set MLS are not shown because they were very similar to the TR four. The near-symmetry of $\mathbf{q}_{s1}$ with $\mathbf{q}_{s4}$ and $\mathbf{q}_{s2}$ with $\mathbf{q}_{s3}$ about the pressure axis in Fig. 5 reflects the near-symmetry of their corresponding cluster centers about the origin in Fig. 4.

The ultimate goal of our retrieval scheme was to determine a given profile's VSC directly from satellite data, without knowing the profile's values of c_2 and c_3 in advance. However, the usefulness of such an exercise depends on whether the four VSCs account for the bulk of the structure information relevant to attendant meteorological conditions.

c. *Meteorological interpretation: A case study*

Statistical tools determined the VSCs, but meteorological application is why they are needed. A case study was used to verify that VSC differences are associated with distinctly different atmospheric conditions.

To obtain a synoptic field of oceanic soundings, we resorted to northwestern Pacific RAOBs. Soundings that fell into the four distinctive classifications of VSC are shown in Fig. 6, and were assigned identification numbers consistent with numbering given in Figs. 4 and 5. Different VSC boundaries were applied south (TR) and north (MLS) of 30°N, but the impact of the difference was small. For meteorological interpretation we also considered daily weather maps (Japan Meteorological Agency, 1982) and composites of imagery from National Oceanic and Atmospheric Administration (NOAA) polar-orbiting satellites (NOAA/EDIS, 1982).

Figure 6 gives an overview of the study case. Spatial consistency and variability are both present, as would be expected in summer, when synoptic-scale circulations are weak and mesoscale circulations give rise to local variations in atmospheric structure. A sample RAOB from each of the four VSCs is shown in skew T–log$p$ format in Fig. 7. The corresponding sounding sites are marked on Fig. 6.

Example 1 (Fig. 7a) was taken in a region of subsidence under a subtropical high pressure ridge, with warm water at the surface. The temperature profile has an elevated, highly stable layer, and the water vapor profile is correspondingly moist near the surface and dry aloft. Example 2 (Fig. 7b) includes a shallow layer of humid air near the surface, with rapid drying up to 70 kPa and a temperature profile that has high potential instability. This sounding site was on the northeast side

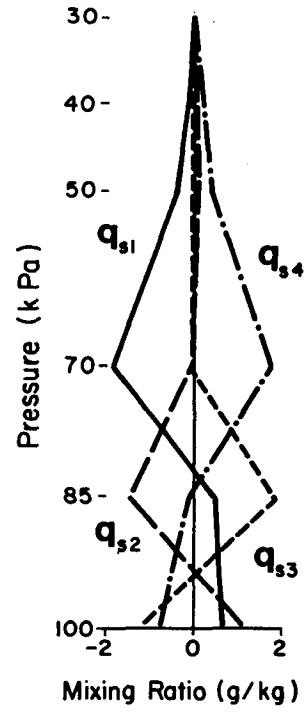

FIG. 5. The mixing ratio profiles associated with the four VSCs. Each one was derived from cluster center coordinates using (5), and is labeled according to the numbering system of Fig. 4.

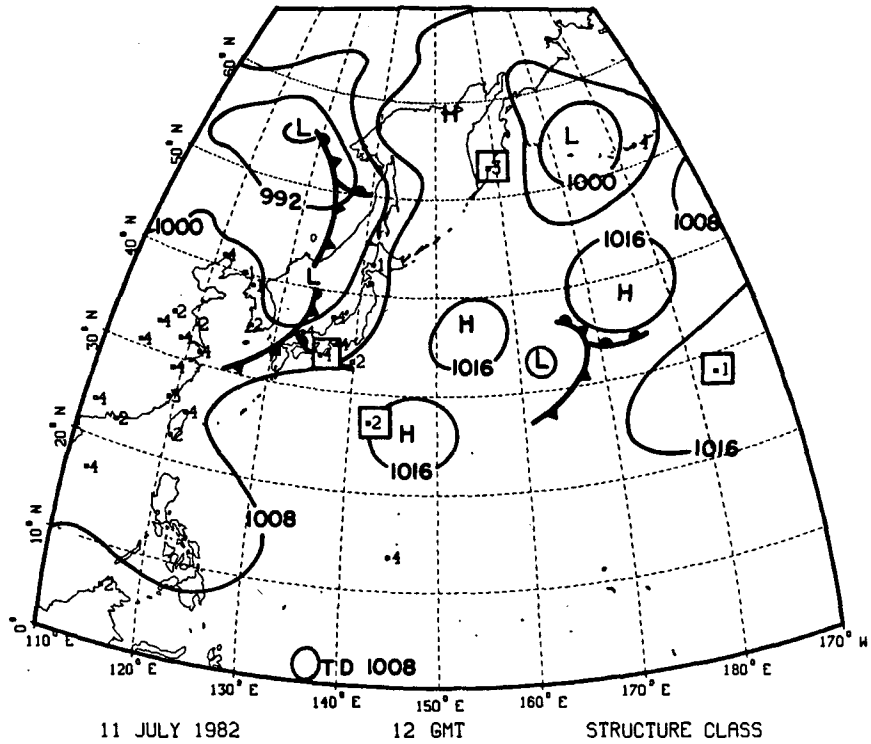

FIG. 6. A plot of VSC identification numbers for radiosonde soundings of mixing ratio, with the numbering system of Figs. 4 and 5. Only the "distinctive" soundings are shown. Surface frontal positions and centers of high (H) and low (L) pressure features are shown for reference; sea level pressure is contoured at 8 mb increments. The boxes indicate soundings plotted in Fig. 7.

of the subtropical ridge. Example 3 (Fig. 7c) came from the rear of an extratropical cyclone where dry polar air was overriding a stratocumulus cloud layer. The dew point temperature varied little between the surface and 85 kPa. Example 4 (Fig. 7d) was taken just in advance of a warm front and exhibits abundant moisture deep into the troposphere.

Not all of the VSC assignments shown in Fig. 6 closely conformed to the meteorological interpretations of the four highlighted examples. However, the examples were representative of the meteorological processes that give rise to particular sounding structures, and show that some meteorological inferences can be drawn from knowing the VSC at a site. The results indicate that the VSC is a useful parameter to seek to retrieve from satellite data.

4. Retrieval

To approximate a water vapor profile, $\mathbf{q}$, from satellite data we must retrieve both $\mathbf{q}_w$ and $\mathbf{q}_s$ (see Eq. 3). We chose to retrieve $\mathbf{q}_w$ by way of c_1 (Eq. 4) through linear regression on satellite brightness temperatures. Regression was used because c_1, the overall wetness principal component, is closely related to the approximate total precipitable water, U (Vonder Haar et al., 1983), and U has been retrieved by regression with high success (e.g., Rosenberg et al., 1983). To retrieve $\mathbf{q}_s$ we chose not to use regression applied to c_2 and c_3 (Eq. 5) (as in Smith and Woolf, 1976), but instead chose to concentrate the information content of the brightness temperatures into estimating which VSC a given sounding belonged to. The VSC was retrieved by discrimination on brightness temperatures. Discrimination is similar to classification except that it relies solely on indirect information (Kendall, 1975).

a. *Retrieval of overall wetness*

Linear regression coefficients were derived by means of the "All Possible Subsets" routine of BMDP (Dixon, 1981). The TR and MLS sets were treated separately, using both RAOBs and simulated brightness temperatures from each set for training and testing the regressions. We used Mallow's C_p criterion (Dixon, 1981) to determine which combination of the 16 SSH-2 channels would be most likely to perform best at retrieving c_1 from an independent dataset, and the adjusted-R^2 parameter to estimate that performance in terms of explained variance.

For the TR set a regression equation including brightness temperatures from seven channels produced

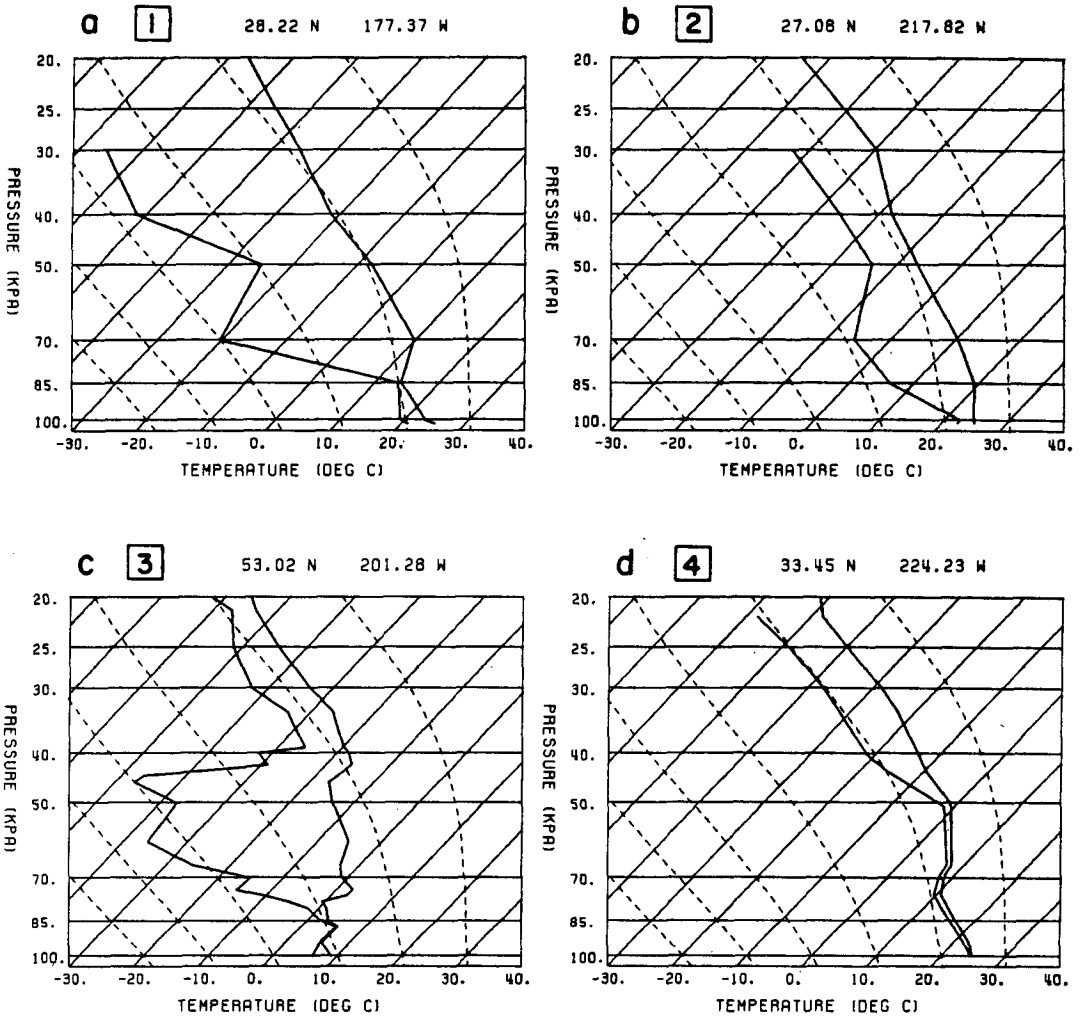

FIG. 7. Radiosonde profiles of temperature and dew-point temperature for 12 GMT, 11 July 1982 at the locations indicated by squares on Fig. 6. Plots a–d were classified as VSCs 1–4, respectively. The dashed curves represent pseudoadiabats.

an adjusted-R^2 of 81%. For the MLS data the results were eight channels and 80%, respectively.

b. *Retrieval of VSC*

The "Stepwise Discriminant Analysis" routine of BMDP (Dixon, 1981) was used to compute discrimination coefficients for retrieving the VSC (classes 1–4) from SSH-2 brightness temperatures. As in the regression step, sets TR and MLS were treated separately. We used forward and then backward stepping to determine which combination of SSH-2 channels was likely to most reliably retrieve the VSC from an independent dataset, using the "leaving-one-out" (LOO) method (Lachenbruch, 1975) as the measure of potential success. This method provides an estimate of the proportion of independent set soundings that will be correctly classified through discrimination.

Before performing discrimination, we divided each dataset into "wet," "medium" and "dry" subsets according to the soundings' "overall wetness." This was done for the following reason. The position and shape of water vapor channel weighting functions are a strong function of the total water vapor content of the viewed atmosphere, as demonstrated by Hayden et al. (1981). The particular response of SSH-2 channels to changes in U will affect how well they detect changes in VSC. For example, in a dry atmosphere, channel F5 (Fig. 1) may be very useful for retrieving the water vapor structure of the lower troposphere, but in a very wet atmosphere that channel may be irrelevant to that purpose, or redundant to other channels. This sensitivity problem suggests that channel selection may be enhanced by deriving separate discrimination coefficients for wet, medium and dry atmospheres. We subdivided our datasets objectively, based on each sounding's

overall wetness parameter, c_1 (Vonder Haar et al., 1983).

Discrimination results for the TR and MLS sets are summarized in Table 2. Results were computed for each set treated as a whole, and for its dry, medium and wet subsets. An average over the three subsets is also shown, and allows for comparison of results for the full set either treated as a whole or as a triplet of subsets. To assess discrimination skill we considered percentages of correct discrimination for dependent data and for independent data (LOO estimate). Also, we considered results for the distinctive sounding segment of the dependent data to determine how much improvement would result from neglecting borderline cases. It should be noted that with four VSCs, random (no-skill) discrimination would produce percentages of about 25%, versus 100% for perfect discrimination.

The distinctive soundings were assigned to the correct VSC slightly more reliably than the full range of soundings were (Table 2). This result indicates that borderline soundings are relatively difficult to discriminate. Conversely, discrimination performs best on relatively distinctive soundings. Also, with respect to the full range of soundings, the subsets (dry, medium, wet) produced higher correct discrimination rates than the whole sets. The same was not true for the distinctive soundings alone. This indicates that the tenuous VSC discrimination of borderline soundings was hindered by large variations in overall wetness within a dataset.

c. *Overview of the retrieval method*

Figure 3 showed how a sounding can be decomposed using EOF analysis. Figure 8 illustrates how our retrieval method can reconstruct this sounding in approximate form. The tropical sounding shown was selected because its retrieval error is typical for the TR

TABLE 2. Retrieval of vertical structure class.

Set	Subset	Number of soundings		Discrimination % correct		
		Full	Dtv[a]	Dep[b]	Ind[c]	DD[d]
TR	—	360	153	55	53	66
TR	Dry	107	46	72	66	74
TR	Medium	145	67	67	61	64
TR	Wet	108	40	57	53	65
TR	Average	360	153	65	60	67
MLS	—	251	75	55	50	65
MLS	Dry	95	19	54	46	74
MLS	Medium	101	35	58	55	54
MLS	Wet	55	21	73	58	62
MLS	Average	251	75	60	52	61

[a] Distinctive soundings
[b] Dependent data
[c] Independent data (LOO estimate)
[d] Dependent data, distinctive soundings only

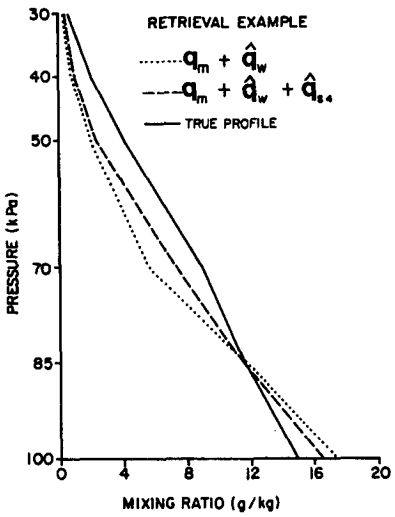

FIG. 8. An example of a water vapor profile retrieval, demonstrating the two-step process. The dotted curve is derived from c_1 via (4) and (3). The dashed curve results from adding the effects of VSC 4 using (3). The carets indicate retrieved quantities. The solid curve is the true profile.

set. First, c_1 was retrieved by regression and used to determine $\mathbf{q}_w$ from (4). The value of c_1 also determined that the sounding belonged to the wet subset. Next, the VSC was retrieved using the TR-wet discrimination equations. The result was VSC 4, directly determining that $\mathbf{q}_{s4}$ was the appropriate structure component to include in the final retrieval product (Fig. 8).

The dotted and dashed curves in Fig. 8 do not differ greatly, but the final result is advantageous in that the discrimination has identified the class of vertical structure present. This information alone could be useful in subjective weather analysis (see section 3c). Also, discrimination has reduced the error of the retrieved profile. For example, for the 360 TR soundings, retrieval of c_1 explained 57.9% of the vertically averaged variance of mixing ratio, whereas subsequent discrimination of vertical structure increased the explained variance to 63.5%.

To give reference to these numbers we applied a slightly modified version of the Smith and Woolf (1976) retrieval method to our TR data, allowing for objective comparison. The Smith and Woolf method produced an averaged explained variance of 69.1%. Apparently, our method is not advantageous as measured by the accuracy of the final retrieved profile. However, the subjective value of identifying the VSC of a profile is not amenable to comparison.

The retrieval scheme reported here incorporates the physics of the retrieval problem in two new ways. First, the inherently poor vertical resolution of water vapor soundings, due to broad weighting functions, is recognized by limiting the possible outcome of the retrieval to four vertical structure classes. Second, the shifting of weighting functions with overall water con-

tent is compensated for by dividing the retrieval procedure into two steps. That is, soundings are separated by approximate total water content before vertical structure information is retrieved. By including these physical considerations in an otherwise statistical retrieval scheme, water vapor profiles may be estimated in a computationally efficient way.

5. Conclusion

A statistically based procedure for retrieving water vapor profiles from satellite data has been developed through two stages of investigation. First, water vapor profiles from a set of oceanic radiosonde observations were decomposed by means of empirical orthogonal function (EOF) analysis, and their components were used to define four classes of vertical water vapor structure that were most characteristic of the sounding sets. A case study indicated that the vertical structure class of a sounding could be used in evaluating meteorological conditions at the sounding site. Second, a retrieval procedure was designed to determine both the overall wetness and the vertical structure classification of any particular profile from satellite brightness temperatures.

The retrieval method was applied to tropical and midlatitude summer radiosonde soundings, in combination with simulated DMSP SSH-2 sounding data. The overall wetness parameter, c_1, was retrieved with explained variances of about 80% by regression. Discrimination was used to retrieve vertical structure class, with expected rates of correct discrimination in the range of about 50–60% for four-class discrimination on independent data. Rates were slightly higher where evaluation was limited to soundings that exhibited especially distinct vertical structure. These percentages should be compared with reference values of 25% for no skill and 100% for complete skill, and should be considered in light of the difficulty of the water vapor retrieval problem. The skill of our method was increased by the separation of soundings into wet, medium and dry subsets, according to c_1, before the discrimination step.

The primary conclusions of this study were as follows.

1) The statistical tools of EOF analysis, clustering and classification can be used to identify classes of water vapor profile vertical structure that differ in a meteorologically significant way.

2) Infrared spectral radiances from satellites can be used to recognize water vapor structure classes as they occur in the atmosphere.

For application to weather analysis, it would be useful to plot the results of satellite soundings on maps similar to Fig. 6. It would also be useful to overlay contours of the total precipitable water estimated from c_1 retrieval. For a case in which real satellite soundings were used, one would expect to have erroneous classifications in the retrieval fields because of discrimination errors. However, the density of measurement would be much greater than for the oceanic radiosonde network, thus allowing for reasonable meteorological interpretation, except in regions where clouds prevent retrievals. This retrieval approach could also be applied at the mesoscale over land, where the radiosonde density is insufficient for mesoscale analysis.

Acknowledgments. We thank Larry Crone and Dr. Mike Weinreb of NOAA/NESDIS for providing the radiosonde profiles used as our data base. We also appreciate the suggestions and assistance of Dr. Stephen Cox and Patrick Laybe. Typing was skillfully done by Loretta Wilson and figure drafting was done by Judy Sorbie.

This research was supported primarily by the Air Force Geophysics Laboratory under Contract F19628-80-C-0140. Additional support was provided by NOAA Contracts NA81RA-H-00001 and NA84AA-H-00020.

REFERENCES

Barnes Engineering Company, 1978a: Special Sensor H-2 (SSH-2) System Analysis Report, 2418-TR-007, 128 pp. [Available from: Barnes Eng. Co., Stamford, CT 06904]

——, 1978b: Flight V Special Sensor H-2 (SSH-2) Radiometric Performance, 2418-TA-010, 119 pp. [Available from: Barnes Eng. Co., Stamford, CT 06904]

Chesters, D., L. W. Uccellini and A. Mostek, 1982: VISSR Atmospheric Sounder (VAS) simulation experiment for a severe storm environment. *Mon. Wea. Rev.*, **110,** 198–216.

Dixon, W. J., Ed., 1981: *BMDP Statistical Software.* University of California Press, Berkeley, 725 pp.

Gruber, A., and C. D. Watkins, 1979: Preliminary evaluation of initial atmospheric moisture from the TIROS-N sounding system. *Satellite Hydrology.* M. Deutsch, D. R. Wiesnet and A. Rango, Eds. American Water Resources Assoc., Minneapolis, MN 55414, 115–123.

Hayden, C. M., W. L. Smith and H. M. Woolf, 1981: Determination of moisture from NOAA polar orbiting satellite sounding radiances. *J. Appl. Meteor.,* **20,** 450–466.

Hillger, D. W., 1984: Spatial and temporal variations in mesoscale water vapor retrieved from TOVS infrared radiances in a nocturnal inversion situation. *J. Climate Appl. Meteor.,* **23,** 704–723.

Jalickee, J. B., and C. F. Ropelewski, 1979: An objective analysis of the boundary-layer thermodynamic structure during GATE. Part I: Method. *Mon. Wea. Rev.,* **107,** 68–76.

Japan Meteorological Agency, 1982: *Daily Weather Maps,* July. Otemachi, Chiyoda-ku, Tokyo, Japan, 250 pp.

Kendall, M., 1975: *Multivariate Analysis.* Hafner Press, 210 pp.

Kneizys, F. X., E. P. Shettle, W. O. Gallery, J. H. Chetwynd, Jr., L. W. Abreu, J. E. A. Selby, R. W. Fenn and R. A. McClatchey, 1980: Atmospheric Transmittance/Radiance: Computer Code LOWTRAN 5, AFGL-TR-80-0067, 233 pp. [NTIS AD A088215]

Koprova, L. I., and M. S. Malkevich, 1965: On the empirical orthogonal functions for the optimal parameterization of temperature and humidity profiles. *Izv. Acad. Sci. USSR Atmos. and Oceanic Phys.,* **1,** 27–32. [English translation **1,** 15–18, by American Geophysical Union, Washington, D.C. 20009.]

Lachenbruch, P. A., 1975: *Discriminant Analysis.* Hafner Press, 128 pp.

Moyer, V., J. R. Scoggins, N. M. Chou and G. S. Wilson, 1978:

Atmospheric structure deduced from routine Nimbus-6 satellite data. *Mon. Wea. Rev.*, **106,** 1340–1352.

National Oceanic and Atmospheric Administration, 1982: *Environmental Satellite Imagery.* NOAA/EDIS, July, Key to Meteor. Records Doc. No. 5.4. [NTIS PB83-124545]

Prabhakara, C., G. Dalu, R. C. Lo and N. R. Nath, 1979: Remote sensing of seasonal distribution of precipitable water vapor over the oceans and the inference of boundary-layer structure. *Mon. Wea. Rev.*, **107,** 1388–1401.

Rosenberg, A., D. B. Hogan and C. K. Bowman, 1983: Satellite moisture retrieval techniques, Vol. 1: Technique development and evaluation. NAVENVPREDRSCHFAC Contractor Rep. CR 83-01(a). [NTIS AD-A126 245]

Smith, W. L., and H. B. Howell, 1971: Vertical distributions of atmospheric water vapor from satellite infrared spectrometer measurements. *J. Appl. Meteor.*, **10,** 1026–1034.

——, and H. M. Woolf, 1976: The use of eigenvectors of statistical covariance matrices for interpreting satellite sounding radiometer observations. *J. Atmos. Sci.*, **33,** 1127–1140.

Thompson, O. E., M. D. Goldberg and D. A. Dazlich, 1985: Pattern recognition in the satellite temperature retrieval problem. *J. Climate Appl. Meteor.*, **24,** 30–48.

Twomey, S., 1966: Indirect measurements of atmospheric temperature profiles from satellites: II. Mathematical aspects of the inversion problem. *Mon. Wea. Rev.*, **94,** 363–366.

Uddstrom, M. J., and D. Q. Wark, 1985: A classification scheme for satellite temperature retrievals. *J. Climate Appl. Meteor.*, **24,** 16–29.

Valovcin, F. R., 1980: DMSP Water Vapor Radiances—A Preliminary Evaluation. Air Force Surveys in Geophysics, No. 432, AFGL-TR-80-0313. [NTIS AD A099305]

Vonder Haar, T. H., D. W. Hillger and A. E. Lipton, 1983: Satellite sounding applications at the synoptic scale and as input to global numerical models. Air Force Geophysics Laboratory, Contractor Rep. AFGL-TR-83-0269. [NTIS AD-A148012]

Wark, D. Q., J. H. Lienesch and M. P. Weinreb, 1974: Satellite observations of atmospheric water vapor. *Appl. Opt.*, **13,** 507–511.